MODELLING FARMLAND TOPOGRAPHY FOR SUITABLE SITE SELECTION OF DAM CONSTRUCTION USING UNMANNED AERIAL VEHICLE (UAV) PHOTOGRAMMETRY

Oluibukun Gbenga AJAYI[1], Mark PALMER[2] and Akporode Anthony SALUBI[3],

[1, 2]Faculty of Environment and Technology
University of the West of England, Bristol,
United Kingdom

[1, 3]Department of Surveying and Geoinformatics,
Federal University of Technology, Minna.
Nigeria

[1]Corresponding Author: ogbajayi@gmail.com,

ABSTRACT

UAV photogrammetry and 3D mapping are gaining fast and wide applications around the world majorly due to the relatively low-cost advantage it offers in the acquisition of high resolution 3D topographic models when compared to LiDAR. This research seeks to demonstrate the applicability of UAV photogrammetry and Geographic Information System (GIS) in modelling the topography of a farm land located in Kwandere community, Lafia, Nasarawa state, Nigeria, for the selection of a suitable site for the construction of an earth-fill dam. The image data was acquired with the aid of a DJI Phantom 2 UAV at 120m flying height, with a 3.61mm camera focal length and at 65% overlap. The acquired images were processed using Agisoft Photoscan digital photogrammetric software and 20 GCPs were used for the georeferencing and check points for accuracy assessment. The Digital Elevation Model (DEM) of the area was generated from the acquired 2D image sequences using Structure from Motion (SfM) techniques, at a horizontal and vertical accuracy that falls within the desirable threshold according to NSSDA standard. Using the hydrologic tool of ArcGIS 10.3.1, the produced DEM together with the contour map of the area was finally used to determine the suitable location for the siting of dam using topographic constraints. The results obtained demonstrates the robustness of UAS products and their usefulness for planning purposes in construction and engineering applications.

Key words: UAV Photogrammetry, UAV Mapping, GIS, Dam-axis, DEM, 3D Topographic Models, Point Cloud.

1.0 INTRODUCTION

Accurate photogrammetric representation and 3D reconstruction of the environment is of great importance to various applications including topographic modelling, mapping, engineering, construction, environmental monitoring, agriculture, etc. Recent advances in hardware and software development has led to the introduction of Unmanned Aerial Vehicles (UAVs) also known as drones for accurate 3D mapping. These utilise low-cost digital cameras and navigation systems, providing high scale, time efficient and low-cost facility for aerial surveying and mapping (Sammartano and Spanò, 2016, Ajayi *et al.*, 2017b, Cook, 2017) especially for areas that are relatively not too large. The traditional approach of using manned aerial vehicles for large scale mapping is quite expensive (Remondino *et al.*, 2011),

so also is the application of Light Detection and Ranging (LiDAR) in manned and unmanned systems for the acquisition of high spatial resolution surface models (Haala and Rothermel, 2012). UAV photogrammetry introduced a low-cost alternative to the time consuming classical manned aerial photogrammetry for large-scale topographic mapping or detailed 3D recording of ground information (Le-Mauff *et al.,* 2018) whilst also being a valid complementary solution to terrestrial acquisitions (Nex and Remondino, 2014). It therefore provides an alternative to the very expensive, yet dominant use of airborne LiDAR for the acquisition of high resolution digital surface models (Zhou *et al.,* 2015). Since UAVs can fly at a lower altitude, they can collect images with an unprecedented level of detail and provide a great opportunity for high-resolution mapping (Colomina and Molina 2014; Hackney and Clayton 2015) which aids quick and direct earth monitoring and tracking of spatio-temporal changes. LiDAR sensors can also be mounted on Drones (Unmanned Airborne Laser Scanning- UALS) which fly at a lower altitude, and as such, enables high-resolution mapping, acquiring topographic details of the earth surface or area of interest using laser pulses. The drawback to this method is the high cost of LiDAR sensors. In contrast photogrammetry allows the utilisation of UAVs to capture a series of aerial images which are then incorporated with spatial data based on GNSS and/or Inertial Measurement Unit (IMU) to produce a high resolution 3D point cloud that can be used for a wide range of geological, civil/mining engineering applications and projects (Tziavou *et al.,* 2018). UAV photogrammetry is a robust technology for 3D mapping, visualisation and modelling, post earthquake quick damage assessment (Baiocchi *et al*., 2013), thus, contributes to applications such as topographic surveys, photogrammetric solutions, disaster risk and management, mapping, precision agriculture, etc. (Zhang and Kovacs, 2012; Tziavou *et al.*, 2018). Very recently and more specifically related to agriculture, the use of UAV has been adopted in plant conservation (Koh and Wich, 2012; Baenaa *et al.,* 2017), vegetation analysis based on spectral-spatial methods (Senthilnath *et al.,* 2017), landscape phenology, vegetation classification, forestry (Torresan *et al.,* 2016), and mapping vegetated areas (Salamí *et al.,* 2014), etc. UAV has also been experimented for civil engineering applications such as mining in quarries (Raeva *et al.,* 2016), determination of stockpile volumes (Draeyer and Strecha, 2014), construction (Siebert and Teizer, 2014), etc.

While the technology of UAV continues to gain wide acceptance in different disciplines, the integrity and reliability of the models or products derivable from it is still a major subject of research. Eltner *et al.* (2014) measured the changes in short term erosion events using rotary-wing UAV acquired images and the outcome of the measurement shows that the DSM generated from the UAV imagery favourably competes with the DSM produced from terrestrial laser scanning data. Eltner also noted that UAV provides advantages in terms of qualifying and quantifying changes of soil surface at field scales. The results obtained by Uysal *et al.* (2015) also affirmed that UAV photogrammetry is a robust technology for mapping, topographic modelling, precision agriculture, etc with advantages such as time economisation, less rigorous field operation, access into inaccessible areas and at a comparatively low cost. Agüera-Vega *et al.* (2017) investigated the effect of using different number of ground control points (GCPs) on the final accuracy of the DEM produced via UAV Photogrammetry. While agreeing that it is important that GCPs be established *a-priori* to the mission and used for image processing in order to obtain reliable DSM for geomatics applications, the research suggested that best results are obtained with the use of 15 – 20 GCPs, especially when an accuracy that is good enough for engineering project applications is required.

Using 20 GCPs, this research seeks to demonstrate the use of UAV in 3D mapping by producing different topographic (3D) models, useable for agricultural planning purpose and more specifically, for the selection of suitable site location for the construction of a earth-fill dam for irrigational purpose, further extending the multi-variate application of UAV imagery in different fields and disciplines. The choice of UAV for this study was also informed by the unavailability of existing large scale cartographic data, existing lidar data, and existing airborne photogrammetric data which can be used to produce a Digital Elevation Model of 1m accuracy.

1.1 DAMS

A dam can be defined as a structure that prevents the flow of water and allows it to accumulate to form a reservoir for water storage (Behrangi, 2001). Earth fill dams are subsurface structures blocking the fluid flow in the earth's layers, leading to water storage in the upper alluvial through the development of an obstacle against groundwater flow. They can be small, medium or large, depending on the volume of water they can retain. The horizontal centre line of a dam in the longitudinal direction is known as the dam-axis, also referred to as the baseline of the dam. It is the line of the upstream edge of the top of the dam, which is always a straight line. It is also defined as the plane surface, arbitrarily chosen by a designer, appearing as a line, in plan or in a cross section, to which the horizontal dimensions of a dam can be referred (www.dnr.wi.gov).

Dams are constructed for various purposes such as domestic water supply, flood control, inland water navigation, hydroelectric power generation, irrigation, etc. Since the construction of dams is always very expensive and as such, due diligence must be observed in the choice of a suitable location for their construction. This is to ensure that the most economic approach is adopted and to minimize chances of dam failure which can lead to loss of life and properties. The factors that should be considered in choosing the site of a dam are multidisciplinary in nature. These factors include the topography of the area, the gradient of the slope, power and rate of flow, the basin's geological structure, environmental impact, hydraulic and hydrological characteristics of the precipitation basin, types, thickness and porosity of the rocks, stability of the slope of the lake, shape and type of the valley, etc (Becue, 2002). For this research, the scope of the study was limited to topographic conditions and related factors.

2 METHODS AND MATERIALS

2.1. STUDY AREA

The study area covers a land mass with an area of approximately 0.81 square kilometres (81 hectares) which is a proposed site for the construction of a small dam to be used for irrigation purposes. It is located within the boundaries of Northings 946,878.624mN and 946,695.027mN and Eastings 439,410.264mE and 440,715.174mE in Shuba/Kwandere community, district of Assakio in Lafia Local Government Area, the community is 11 km away from Lafia, the capital city of Nasarawa state, North-central, Nigeria, referenced to WGS1984, Minna datum coordinate reference system. The terrain configuration of the study area is quite even; neither too gentle nor too rugged. The land is largely water logged with streams flowing between two slope gradients and is notable for rice farming together with other crops such as maize, palm plantation and a few mango trees. With plans of the Nasarawa State Government to increase the annual production of rice, a dam would increase the size of arable land for the cultivation of rice and for the irrigation of other arable lands for the plantation of other crops such as sugar cane, palm, guinea corn, maize etc (fig 1).

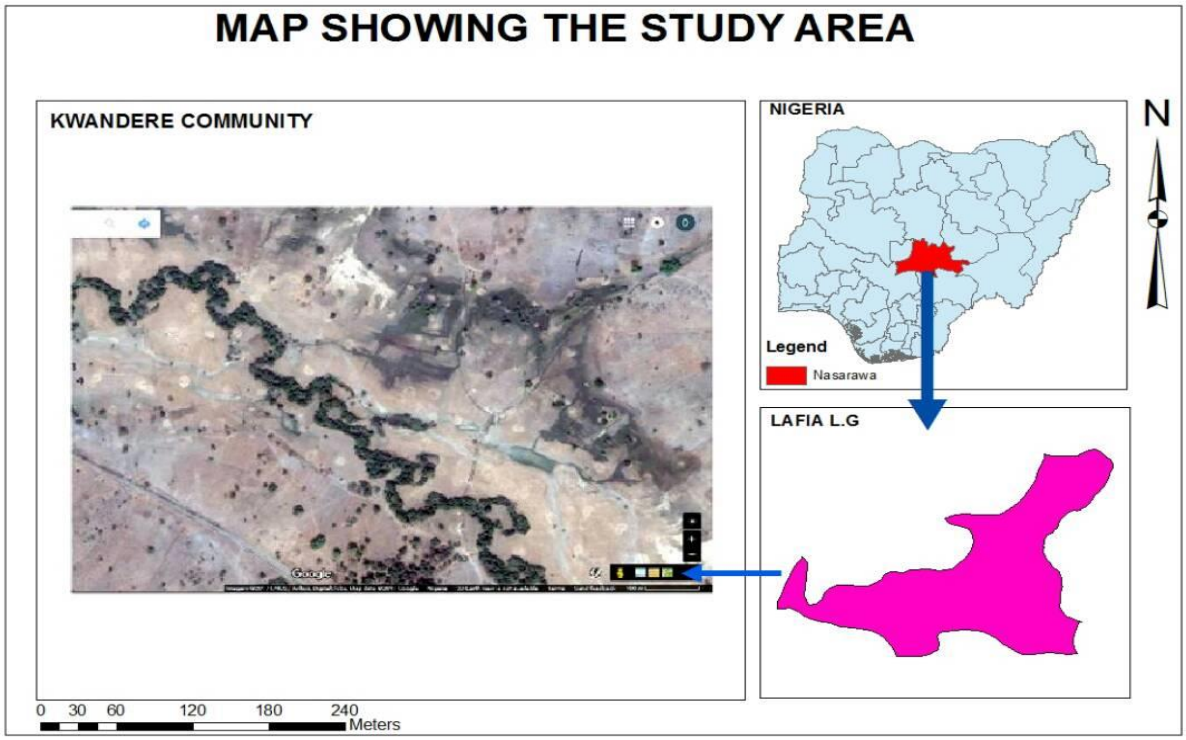

Figure 1: The Study area.

2.2. SITE RECONNAISSANCE AND FLIGHT PLANNING

The reconnaissance was subdivided into two parts which were conducted on site and remotely in the office. During the field reconnaissance, the UAV was used to acquire video of the study area. This was later used during the office reconnaissance to determine suitable locations for the establishment of ground control points (GCPs), and to prepare a working flight plan. The video also helped in deciding the appropriate flying height to get optimal image overlaps (sidelaps and endlaps). Figure 2 presents the flight plan which was used for the image data acquisition.

2.3. IMAGE /DATA ACQUISITION

Before conducting the flight mission, stations pre-marked during the reconnaissance for the establishment of GCPs were positioned using two units of Hi-Target Differential Global Positioning System (DGPS) receivers with one serving as a base station (permanently stationed) while the other was roving over the GCPs and positional data acquired in Real Time Kinematic (RTK) mode. The distance between the base station and the rover is approximately 900 m. A total of 20 GCPs were established across the imaging area (see Figure 3). These GCPs are important for accurate georeferencing of the images (to ensure precise alignments), removal of the effects of bowling in the UAV data (Mesas- Carrascosa et al., 2015) and also for qualitative analysis of the expected 3D model. After calibrating the UAV and ensuring that all its parts are in perfect working condition, and also setting all parameters on the DJI GO mapping made easy map pilot app, the area to be mapped was defined and the controller was connected to the drone, the nadir images were captured autonomously using DJI phantom 2 quadcopter equipped with a GoPro 3 camera model, with camera focal length of 3.61mm at 120m flying height and camera sensor width of 6.17 mm. The camera frame pixel size of each of the acquired overlapping images is 4000 × 3000 mm, covering approximately 34,090.68 m^2 (0.0341 km^2) on the ground, with approximately 65% overlap to ensure stereoscopic imaging.

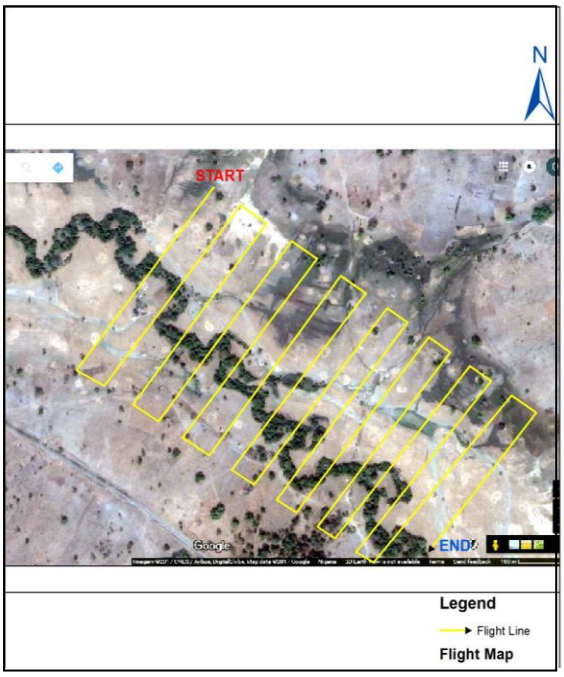

Figure 2: Flight plan

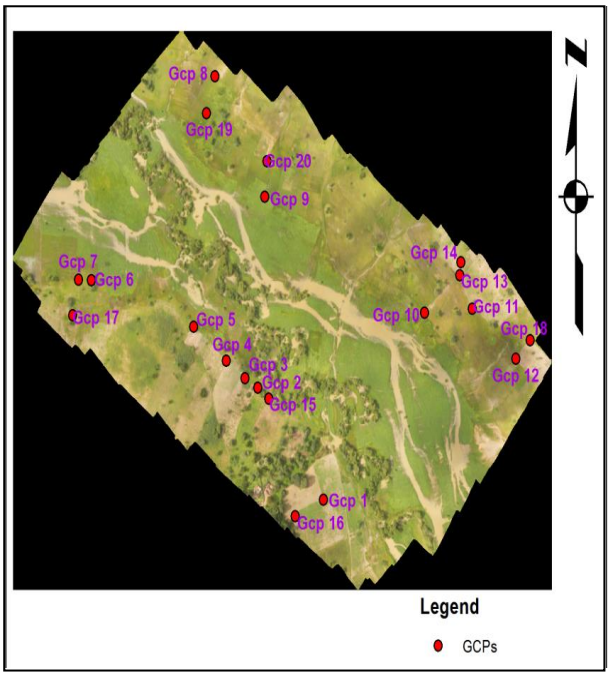

Figure 3: Distribution of the used GCPs

2.4 DATA PROCESSING AND VALIDATION

All the acquired overlapping images were processed using Agisoft Photoscan digital photogrammetric software. The processing involves relative orientation/external orientation, interior orientation, absolute orientation and the generation of 3D models from the 2D acquired image sequences using Structure from Motion (SfM) photogrammetric range imaging technique (Ullman, 1979; Westoby *et al.*, 2012). Figure 4 presents the process flow diagram of the photogrammetric processing of the UAV acquired images into different products in Agisoft Photoscan software environment.

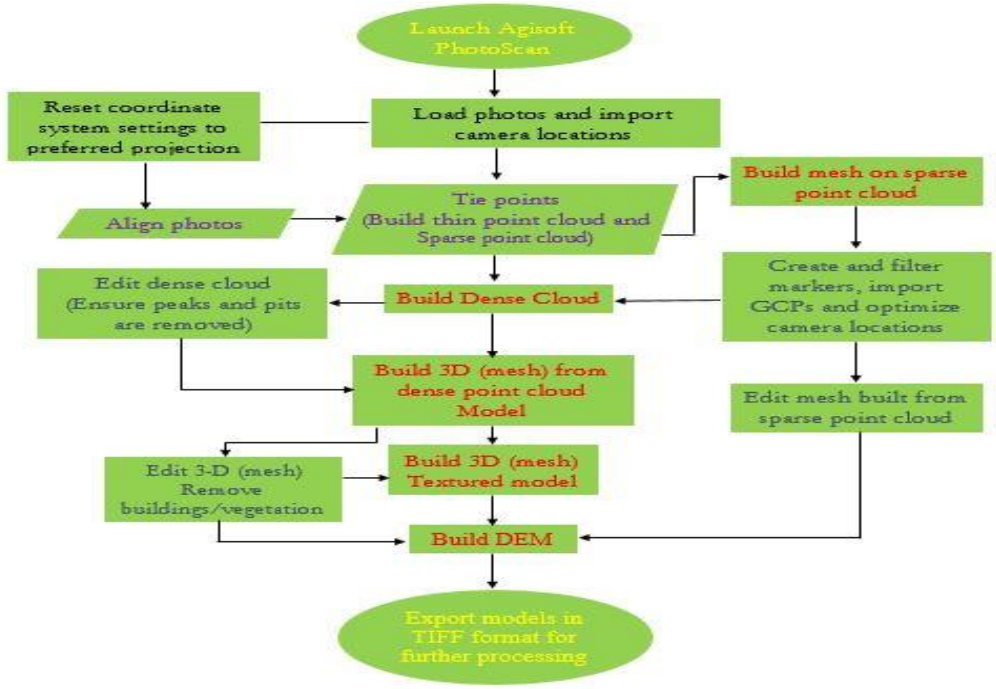

Figure 4: Work flow of the photogrammetric image processing in Agisoft Photoscan

The final products generated from the photogrammetric processing are the Digital Surface Model (DSM) and the Digital Elevation Model (DEM) which was imported as an input parameter into ArcGIS 10.3.1 for further processing which requires the imposition of topographic constraints on the DEM for the determination of suitable locations for the construction of dam-axes within the study area.
For the DEM accuracy assessment, 20 GCPs were coordinated on the ground with the aid of Hi-Target GNSS receivers. Each of these points were pre-marked with a reflective object before the flight mission such that they could be seen on the acquired images. The coordinates of these points were later extracted directly from the produced orthophoto/DEM. The extracted coordinates were compared with the GNSS acquired coordinates. The discrepancy between the measured data and the extracted data (from UAV produced DEM) was estimated and used for the computation of Root Mean Square Error (RMSE), the horizontal and vertical accuracy.

The RMSE was calculated using the formula given in equation (1):

$$RMSE = \sqrt{\frac{\sum(N_i - N_j)^2}{n}} \quad (1)$$

Where N_i is the observed values, N_j is the reference values and n is the number of points (Ajayi *et al*., 2017a).
The horizontal and vertical accuracy were also computed by applying 95% confidence level to the result obtained using the methodology from Geospatial Positioning Accuracy, Part 3 of the National Standard for Spatial Data Accuracy (NSSDA) as presented in equations (2) and (3) respectively (Barry and Coakley, 2013):

$$\text{Horizontal Accuracy} = \mathbf{1.7308} \times \mathbf{RMSE_r} \quad (2)$$

$$\text{Vertical Accuracy} = \mathbf{1.96} \times \mathbf{RMSE_Z} \quad (3)$$

Where $\mathrm{RMSE_r}$ and $\mathrm{RMSE_Z}$ are the Root mean square errors of the horizontal and vertical discrepancy respectively computed using equation (1). The horizontal and vertical accuracy obtained was then compared with the average and maximum allowable misclosure according to NSSDA. The average and maximum horizontal (x and y) allowable limit was computed as Avg (x and y) = 1 x GSD and Max (x and y) = 1.6 x GSD respectively while the average and maximum vertical (z) allowable limit was computed as Avg (z) = 1.6 x GSD and Max (z) = 2.5 x GSD, where GSD is the Ground Sampling Distance which was computed as 10.91 cm.

2.5 SUITABLE SITE SELECTION FOR DAM CONSTRUCTION

Based on the generated DEM, different hydro-topographic models showing the fill map, flow direction, flow accumulation, and stream order maps were produced before finally generating a model showing the suitable locations for the construction of dams as defined by the dam-axes. The flowchart of the GIS modelling is presented in Figure 5.

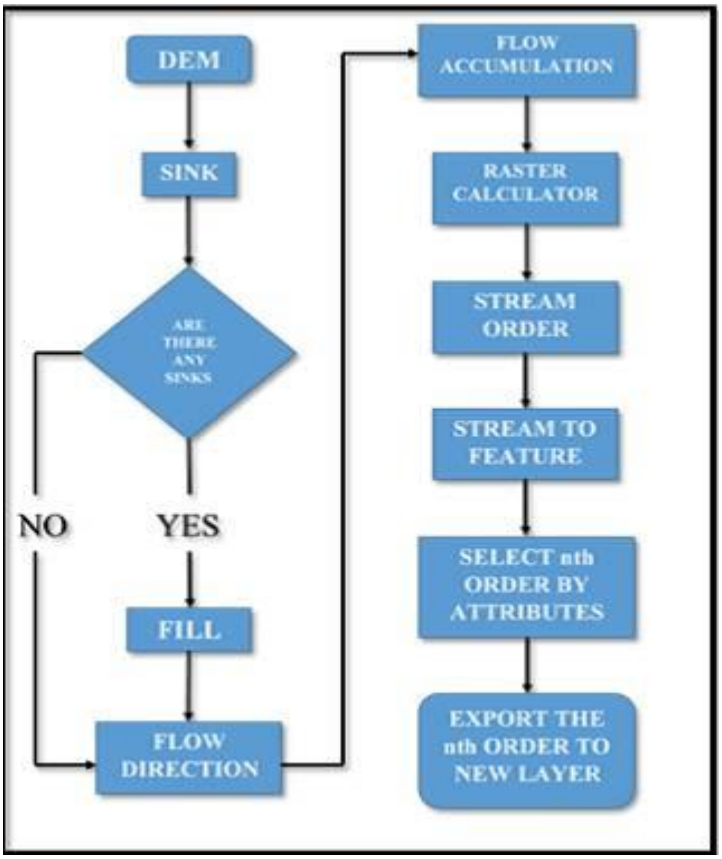

Figure 5: Process flow chat of GIS processing for the suitable site selection of the dam-axes

The DEM was imported into the ArcGIS 10.3.1 software environment and the hydrologic tool was engaged. The first operation carried out was to check for sink(s) on the DEM and to fill them. Sink can be described as a cell or set of cells with an elevation value that is lower than the elevation of its neighbouring cells. The flow direction was then generated using the eight-direction pour point algorithm which assigns a code to each cell based on the steepest downhill slope as defined by the DEM. A flow accumulation map was also generated showing the measure of the drainage area in units of grid cells. The flow accumulation is computed as the accumulated weight of every cell that flows into each downslope cell in the raster image. In the event that no weight raster is provided, a weight of 1 is applied to each cell and the value of cells in the output raster is the number of cells that flows into each cell. Cells with a high flow accumulation are areas of concentrated flow and may be used to identify stream channels and to generate stream order. Cells with a flow accumulation of 0 are local topographic highs and may be used to identify ridges (pro.arcgis.com).

In order to determine the suitable location(s) for siting an earth fill dam in terms of landscape suitability within the study area, the following factors were considered to be significant indicators of the most suitable location (s) within which a dam could be sited or constructed within the study area.

1. Flow direction: A dam-axis must be perpendicular to the direction of flow.
2. Flow accumulation: A dam-axis must obstruct the flow direction in such a manner that will ensure adequate flow accumulation.
3. A dam-axis should be within a V-shaped valley with preferably equal height values at both ends. This will make diversion of water less rigorous by making the accumulation to be in between the points.

3.0 RESULTS AND ANALYSIS

After the photogrammetric processing of the acquired image data, the following 3D models were generated: Sparse point clouds (Figure 6), dense point cloud (Figure 7), Orthophoto (Figure 8), Digital Surface Model (Figure 9) and the Digital Elevation Model (Figure 10). Others are the contour map of the DEM and the vector map showing magnitude and direction of flow. The sparse point cloud (Figure 6) that was generated by triangulation (Snavely *et al.*, 2006), could be described as a representation of rendered set of data points; however, these have limited usage in 3D applications and as such, dense point cloud (Figure 7) must be generated from it by surface and depth reconstruction (Furukawa and Ponce, 2006, Ajayi *et al*., 2017a).

The orthophoto was produced through the aerial triangulation process based on measurement of tie points. It is the image of the scene having successfully registered each of the overlapping image pairs of the study area acquired by the UAV, and also ensuring that both the height and tilt distortions are removed (orthorectification), to ensure geometric correctness which is very important for the accurate extraction of spatial information of the imaged area from the orthophoto. The DSM and DEM are sometimes used interchangeably though they have distinct differences. While the DSM is the surface model which includes terrain model and the surface features visible in the study area, the DEM presents the digital depiction of the earth's surface. The DSM is more useful for urban planning (landscape modelling) while the DEM is good for relief modelling which made it a suitable choice as the input parameter or base map for the identification of suitable dam-axes. The elevation range of the DSM is from 224.964m (lowest point) to 283.588m (highest point) whilst the elevation range of the surface as observed from the DEM is from 224.964m to 268.445m. The variation observed in the elevation value of the highest point is as a result of the difference in features depicted by both models (DSM and DEM). The highest height value of the DSM includes the height of vegetation and natural features visible on the surface of the study area such as trees.

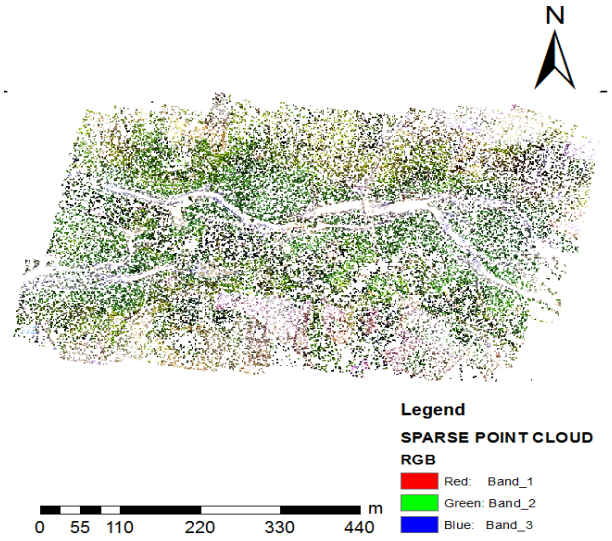

Figure 6: Sparse point cloud

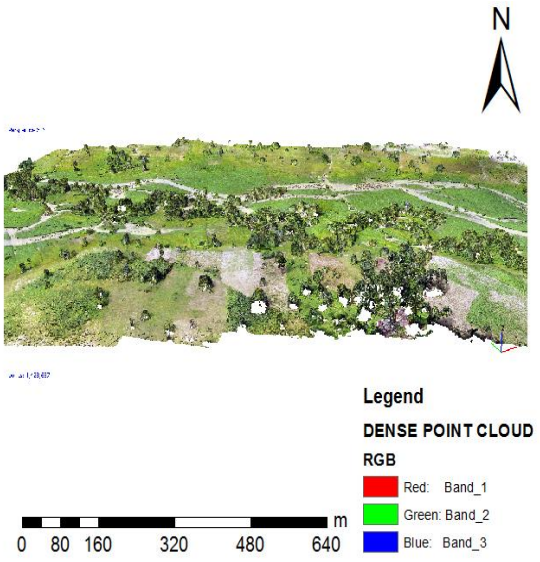

Figure 7: Dense point cloud

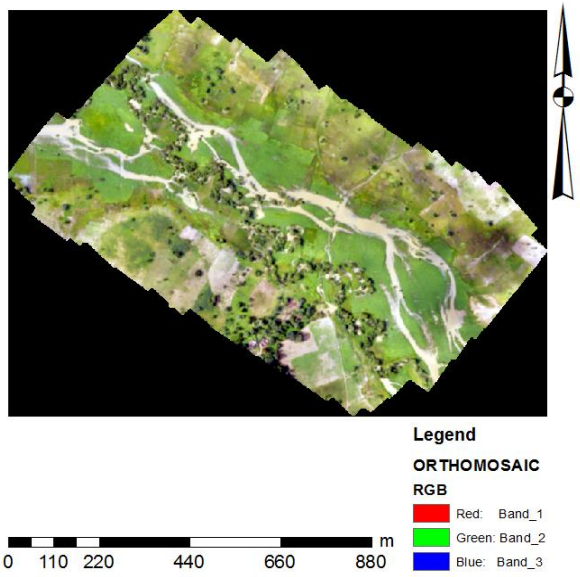

Figure 8: Digital Orthophoto

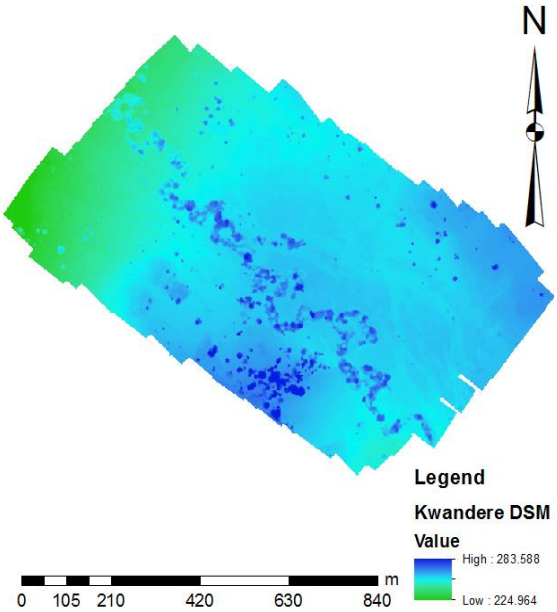

Figure 9: Generated Digital Surface Model

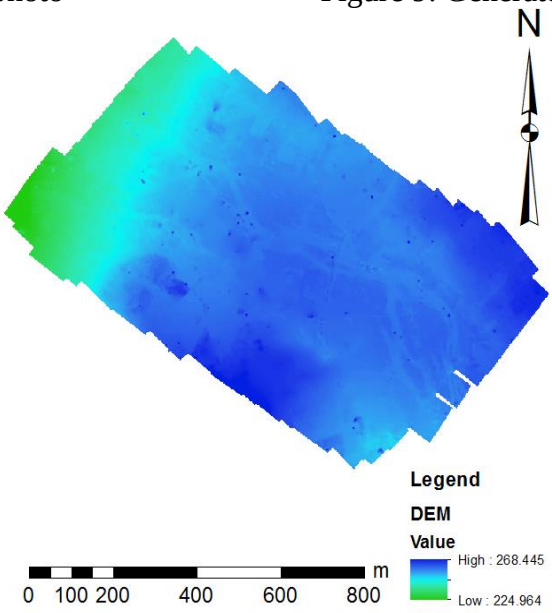

Figure 10: Generated Digital Elevation Model

3.1 RESULTS OF THE MODEL PRECISION ASSESSMENT FOR THE GENERATED DEM

Table 1 presents the discrepancy between the DEM extracted coordinates and the GNSS acquired coordinates. From the table, ΔE(m), ΔN(m) and ΔZ(m) represents the difference in easting coordinates, northing coordinates and the height values respectively as obtained from the DGPS acquired and orthophoto/DEM extracted coordinates of the GCPs. The horizontal (Eastings and Northings) RMSE computed using equation (1) and the discrepancy values recorded in Table 1 is 0.0523 and 0.0443 for the eastings and northings respectively while the computed vertical RMSE using the summation value of ΔZ(m) presented in Table 1 is 0.4687. The computed horizontal accuracy is 0.1186 m while the computed vertical accuracy is 0.9187 m which falls within the acceptable range of accuracy for spatial planning, designs and for engineering projects (Agüera-Vega *et al.*, 2017; Lawali and Dauda, 2014).).

Station ID	Coordinate Discrepancy between GPS coordinate and DEM extracted coordinate values		
	ΔE(m)	ΔN(m)	ΔZ(m)
GCP1	0.166	-0.101	0.215
GCP2	-0.012	-0.109	0.189
GCP3	0.056	-0.038	0.111
GCP4	-0.064	-0.011	-0.128
GCP5	-0.096	-0.036	0.002
GCP6	-0.198	0.041	0.337
GCP7	-0.001	0.105	-0.022
GCP8	-0.166	0.094	-0.514
GCP9	-0.269	0.062	-0.387
GCP10	-0.040	0.029	0.409
GCP11	-0.035	-0.001	-0.215
GCP12	0.188	-0.046	-0.030
GCP13	-0.073	-0.003	-0.054
GCP14	0.095	-0.026	-0.130
GCP15	-0.024	0.113	-0.014
GCP16	-0.119	0.176	-0.159
GCP17	0.220	-0.078	0.720
GCP18	-0.377	0.069	0.771
GCP19	0.196	-0.071	0.381
GCP20	0.279	0.029	0.614
SUM	**-0.234**	**0.198**	**2.096**

Table 1: Differences between GPS acquired and DEM extracted coordinates

3.2 SELECTION OF SUITABLE LOCATION FOR DAM CONSTRUCTION

The dam-axis is expected to be situated within the neighbourhood of very deep stream lines so that the dam can have sufficient depth (with minimal excavation) for adequate water accumulation.

In all, three (3) different dam-axes were generated having met the topographic conditions imposed as earlier discussed in subsection 2.5 and the result is presented in Figure 11. The beginning nodes and end nodes (two edges) of the three dam-axes are of equal elevation values. The first dam-axis which is the shortest of the three, measures 459.622 m in length whilst the height values at both ends are 252.8 m. The second dam-axis is 523.07 m long and the height values at both ends is 252.8 m. The longest axis of the measure 544 m in length with 244.01 m height values at both edges.

The three dam-axes were sited in locations of very deep stream orders, they have equal elevation values both at the beginning nodes and end nodes to ensure a V-shaped valley is easily formed during construction and for adequate water accumulation. The dam-axes are also perpendicular to the direction of water flow so that the flow can be easily dammed.

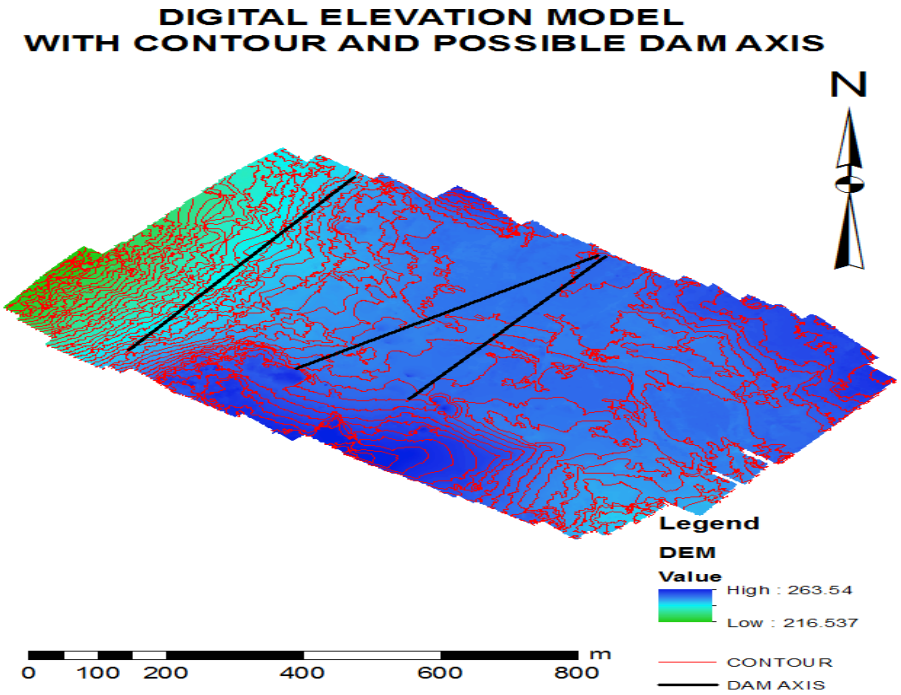

Figure 11: Suitable dam-axes and the contour superimposed on the DEM of the area

4.0 CONCLUSION

This research has demonstrated the applicability of UAV photogrammetry in GIS applications with specific emphasis on selection of suitable site for dam construction. It has also proved that UAV imagery, although a comparatively low-cost technology, is robust enough to produce 3D models. The accuracy obtained is comparable with that obtainable from terrestrial surveying approaches, Manned Aerial Vehicles and LiDAR data all of which are more expensive. A DJI Phantom 2 UAV (Quadcopter) with a GoPro3 camera type was used for the image data acquisition and a DEM was produced from the acquired overlapping images together with some other by-products such as the sparse point cloud, the dense point cloud, generated 3D model (shaded mode and wireframe), textured model, DSM, and Orthophoto. RMSE (Horizontal and vertical), planimetric and vertical accuracy according to NSSDA were used to evaluate the accuracy measure of the generated DEM. The obtained accuracy falls within the acceptable range for planning, designs and extraction of spatial information according to NSSDA standard (Daramola *et al.*, 2017). The produced DEM was finally used to determine the suitable site for dam construction within the study area using topographic constraints. The results obtained shows that UAV photogrammetry is a robust technology for GIS applications and production of 3D surface models to be used for engineering construction designs and planning purposes (Tziavou *et al.*, 2018). Further research efforts shall attempt to investigate the possibility of improving the accuracy of UAV generated DEMs using oblique imageries together with the nadir imageries that were solely used in this research, which is expected to reduce systematic error inherent in the models (James and Robson, 2014; Harwin *et al.*, 2015). This will expand the scope of the multivariate applications of UAV data products into first order control, mapping and engineering projects where high accuracy is needed.

FUNDING
This research did not receive any specific grant from funding agencies in the public, commercial, or not-for-profit sectors.

REFERENCES

Agüera-Vega, F., Carvajal-Ramírez, F., Martínez-Carricondo, P., 2017. Assessment of photogrammetric mapping accuracy based on variation ground control points number using unmanned aerial vehicle. *Measurement* 98, 221–227.

Ajayi, O. G., Salubi, A. A., Angbas, A. F., Odigure, M. G., 2017a. Generation of accurate digital elevation models from UAV acquired low percentage overlapping images. *International Journal of Remote Sensing*, 8-10(38), 3113-3134.

Baenaa, S., Doreen S. Boydb, D. S., Moata, J., 2017. UAVs in pursuit of plant conservation - Real world experiences. *Ecological Informatics*, https://doi.org/10.1016/j.ecoinf.2017.11.001

Baiocchi, V., Dominici, D., Mormile, M., 2013. UAV application in post – seismic environment, International Archives of the Photogrammetry, Remote Sensing and Spatial Information Sciences, XL-1/W2, 21-25, https://doi.org/10.5194/isprsarchives-XL-1-W2-21-2013.

Barry, P., Coakley, R., 2013. Accuracy of UAV photogrammetry compared with network RTK GPS. International Archives of the Photogrammetry, Remote Sensing and Spatial Information Sciences, 2, 27–31.

Becue, J., 2002. Choice of site and type of dam. Chapter One. Available online at: http://www.barrages-cfbr.eu/BackUp/Info/documentation/texte/pb2002/anglais/pb2002-c1-p17.pdf (accessed 15 February 2018)

Behrangi, A., 2001, Underground Dams, A Road Leading to development of Groundwater Resources and Fighting Water Crisis" 1st National Conference on Coping Strategies against Water Crisis, University of Zabol.

Colomina, I., Molina, P., 2014. Unmanned aerial systems for photogrammetry and remote sensing: a review. *ISPRS J. Photogramm. Remote Sens*. 92, 79–97. http://dx.doi.org/ 10.1016/j.isprsjprs.2014.02.013.

Cook, K.L., 2017. An evaluation of the effectiveness of low-cost UAVs and structure from motion for geomorphic change detection. *Geomorphology* 278:195–208. https://doi.org/10.1016/j.geomorph.2016.11.009.

Daakir, M., Pierrot-Deseilligny, M., Bosser, P., Pichard, F., Thom, C., Rabot, Y. Martin, O., 2017. Lightweight UAV with on-board photogrammetry and single-frequency GPS positioning for metrology applications. *ISPRS Journal of Photogrammetry and Remote Sensing 127*, 115–126.

Daramola, O., Olaleye, J., Ajayi, O. G., Olawuni, O., 2017. Assessing the geometric accuracy of UAV-based orthophotos. *South African Journal of Geomatics*, 6 (3), 395-406. Doi*: http://dx.doi.org/10.4314/sajg.v6i3.9*

Draeyer, B., Strecha, C., 2014. White paper: how accurate are UAV surveying methods? Available at: https://support.pix4d.com/entries/40219303-How-accurate-are-UAVsurveying-methods (accessed 15 February, 2018).

Eltner, A. Baumgart, P., Maas, H., Faust, D., 2014. Multi-temporal data for automatic measurement of rill and interrill erosion on losses soil, *Earth Surface Process. Land*. 40 (6), 741–755.

Furukawa, Y., Ponce, J., 2007. Accurate, dense, and robust multiview stereopsis. In CVPR, 2007.

Haala, N., Rothermel, M., 2012. Dense Multi-Stereo Matching for High Quality Digital Elevation Models. *PFG Photogrammetrie, Fernerkundung, Geoinformation*. (4), 331–343.

Harwin, S., Lucieer, A., Osborn, J., 2015. The impact of the calibration method on the accuracy of point clouds derived using unmanned aerial vehicle multi-view stereopsis. Remote Sensing, 7(9), 11933–11953. doi:10.3390/rs70911933

James, M.R., Robson, S., 2014. Mitigating systematic error in topographic models derived from UAV and ground-based image networks. Earth Surface Processes and Landforms, 39(10), 1413–1420. doi:10.1002/esp.v39.10

Koh, L.P., Wich, S.A., 2012. Dawn of drone ecology: low-cost autonomous aerial vehicles for conservation. *Trop. Conserv. Sci*. 5, 121–132 Doi:wos:000310846600002.

Lawali, R., Waziri A. D., 2014. Digital Orthophoto Generation with Aerial Photographs. Academic Journal of Interdisciplinary Studies. 3, 2281-3993.

Le Mauff, B., Juigner, M, Antoine, B., Marc, R., Launeau, P., Fattal, P., 2018. Coastal monitoring solutions of the geomorphological response of beach-dune systems using multi-temporal LiDAR datasets (Vendée coast, France). *Geomorphology* 304, 121–140

Mesas-Carrascosa, F., Torrres-S ánchez, J., Clavero-Rumbao, I., Garcia-Ferrer, A., Pen, J., Borra-Serrano, I., Lopez-Granados, F., 2015. Assessing Optimal Flight Parameters for Generating Accurate Multispectral Orthomosaics by UAV to Support Site-Specific Crop Management. *Remote Sens.* 7, 12793-12814. http://dx.doi.org/10.3390/rs71012793.

National Standard for Spatial Data Accuracy (NSSDA), 1998 "Geospatial Positioning Accuracy Standards." Virginia: Federal Geographic Data Committee.

Nex, F., Remondino, F., 2014. UAV for 3D mapping applications: a review. *Applied Geomatics*. 6:1–15. DOI: 10.1007/s12518-013-0120-x.

Oluibukun Gbenga Ajayi, Ifeanyi Jonathan Nwadialor, Ifeanyi Chukwudi Onuigbo, Olurotimi Adebowale Kemiki., 2017b. Effect of camera calibration on the accurate generation of digital elevation models from UAV acquired low percentage overlapping images. Sustainable Development Goals: A time for innovation and investment in land administration and management. *Commonwealth Association of Surveying and Land Economics (CASLE) International Conference*, 10-11th August, 2017, Dar es Salaam, Tanzania, 108-120.

Raeva, P.I., Filipova, S.L., Filipov, D.G., 2016. Volume computation of a stockpile-a study case comparing GPS and UAV measurements in an open pit quarry. Int. Arch. Photogramm. Remote. Sens. Spat. Inf. Sci. XLI-B1, 999–1004

Remondino, F., Barazzetti, L., Nex, F., Scaioni, M., Sarazzi, D., 2011. UAV photogrammetry for mapping and 3D modeling – Current status and future perspectives –International Archives of the Photogrammetry, Remote Sensing and Spatial Information Sciences, Vol. 38(1/C22), ISPRS ICWG I/V UAV-g (Unmanned Aerial Vehicle in Geomatics) conference, Zurich, Switzerland.

Salamí, E., Barrado, C., Pastor, E., 2014. UAV flight experiments applied to the remote sensing of vegetated areas. *Remote Sens.* 6, 11051–11081. http://dx.doi.org/10.3390/rs6111105.

Sammartano, G., Spanò, A., 2016. DEM Generation based on UAV Photogrammetry Data in Critical Areas. *In Proceedings of the 2nd International Conference on Geographical Information Systems Theory, Applications and Management (GISTAM 2016),* 92-98.

Senthilnath, J., Kandukuri, M., Dokania, A., Ramesh, K. N., 2017. Application of UAV imaging platform for vegetation analysis based on spectral-spatial methods. *Computers and Electronics in Agriculture* 140, 8–24.

Siebert, S., Teizer, J., 2014. Mobile 3D mapping for surveying earthwork projects using an unmanned aerial vehicle (UAV) system. Autom. Constr. 41, 1–14.

Snavely, N., Seitz, S. M., and Szeliski, R., 2006. Photo tourism: Exploring photo collections in 3d. In ACM Transactions on Graphics, 835–846.

Torresan, C., Berton, A., Carotenuto, F., Di, S.F., Gioli, B., Matese, A., Miglietta, F., Zaldei, A., Wallace, L., Torresan, C., Berton, A., Carotenuto, F., Di, S.F., Gioli, B., Matese, A., Miglietta, F., Vagnoli, C., Torresan, C., Berton, A., Carotenuto, F., 2016. Forestry applications of UAVs in Europe: a review of forestry applications of UAVs in Europe: a review. *Int. J. Remote Sens*. 0, 1–21. http://dx.doi.org/10.1080/01431161.2016. 1252477.

Tziavou, O., Pytharouli, S., Souter, J., 2018. Unmanned Aerial Vehicle (UAV) based mapping in engineering geological surveys: Considerations for optimum results. *Engineering Geology* 232, 12–21.

Ullman, S., 1979. The interpretation of structure from motion. *The Royal Society*. 1979. doi:10.1098/rspb.1979.0006

Uysal, M., Toprak, A.S., Polat, N., 2015. DEM generation with UAV Photogrammetry and accuracy analysis in Sahitler hill, *Measurement* 73, 539–543.

Westoby, M. J., Brasington, J., Glasser, N. F., Hambrey, M. J., and Reynolds, J. M., 2012. Structure-From-Motion Photogrammetry: A Low-Cost, Effective Tool for Geoscience Applications. *Geomorphology* 179: 300–314. doi:10.1016/j.geomorph.2012.08.021.

Zhang, C., Kovacs, J.M., 2012. The application of small unmanned aerial systems for precision agriculture: a review. Precis. Agric. 13, 693–712. http://dx.doi.org/10.1007/s11119-012-9274-5.

Zhou, Y., Parsons, B., Elliott, J. R., Barisin, I., and Walker, R. T., 2015. Assessing the Ability of Pleiades Stereo Imagery to Determine Height Changes in Earthquakes: A Case Study for the El Mayor- Cucapah Epicentral Area. *Journal of Geophysical Research: Solid Earth*, 120:8793–8808.